Time-Efficient Behavioral Modeling of Switched Reluctance Machines

Zichao Jin, Ziyan Zhang, Chengxiu Chen, Selin Yaman, Mahesh Krishnamurthy
Electric Drives and Energy Conversion Laboratory
Illinois Institute of Technology, Chicago, IL 60616 USA
EML: kmahesh@iit.edu; URL: http://drives.ece.iit.edu

***Abstract* — This study presents a time-efficient modelling approach for dynamic behavior and efficiency analysis of a Switched Reluctance Machines (SRM). It employs a hybrid model combining Simulink, finite element analysis (FEA), and hardware measurements to create an accurate behavioral model of the machine. In order to enhance accuracy of the estimated performance, Steinmetz equation is employed to characterize core loss in the machine across different operating points. This approach serves as a template for developing a time-efficient model to analyze performance of any SRM with a high degree of accuracy. Simulation and experimental results are used to show effectiveness of the proposed approach.**

***Keywords* — Switched relucatance machine, behavioral model, core loss, finite element methods, electric motors.**

I. INTRODUCTION

Switched reluctance motors (SRMs) have received a lot of attention in recent years owing to several inherent advantages including simple and low-cost construction; robustness under harsh condition (mechanical and thermal); high power density; wide operating speed range and reliability in several automotive, locomotive and aerospace applications [1]. It is well understood that analysis of dynamic behavior of an SRMs can be challenging due a highly nonlinear relationship between inductance, phase current, and rotor position [2]. In order to implement a drive system of SRMs for high performance applications such as vehicle propulsion, an accurate and time-efficient model needs to be developed for calculating optimal turn-on and turn-off angles, developing fault-tolerant strategies, implementing advanced sensorless control approaches and for effective real-time control methods.

Most existing SRM models are based on pre-defined inductance/flux linkage characteristics that are extracted from the measurements from a machine prototype [3-7], finite element analysis [8-10]. Although methods based on experimental measurements are often more accurate in the characterizing magnetic characteristics, they can not be used for the fundamental electromagnetic design of the machine itself. On the other hand, methods based on FEA can be used during the design stage and are therefore more effective in the manufacturing or prototype stages. Normally, the pre-calculated magnetic relationships from FEA can be used as look-up table (LUT) or analytically reconstructed with mathematical approaches to build the dynamic model. Magnetics circuit modelling approach has been another hotspot for researchers, and several studies have utilized this approach [11-15]. Analytical modeling techniques have lower computational intensity, but design of a controller using a complex expression can be challenging [16]. LUT based methods are generally more accurate and suitable for both analyzing the SRM and designing of control algorithm without being computationally intense like purely FEA methods. Another approach for SRM modeling uses artificial-intelligence techniques such as neural networks [17]. Although they have a high potential for accuracy and repeatability in SRM analysis, their practical value is limited due to high complexity and computation time.

Majority of existing SRM models focus the flux linkage, inductance, and output torque without developing an accurate model to estimate efficiency as a including core losses and material properties. For practical calculation of efficiency, it has been established that the core losses in the machine need to be included in addition to the ohmic losses.

This paper presents a modelling approach for High-Rotor Switched Reluctance Machines (HRSRM), where the number of rotor poles is higher than the number of stator pole, this type of SRM has higher torque density, comparable torque ripple, and lower manufacturing costs compared to a conventional SRM with identical number of phases with same power electronic circuit [18-19]. It presents a time-efficient electromagnetic model that can be used to develop advanced control strategies for multi-objective optimization. Using this method, both dynamic performance and efficiency can be predicted accurately in relatively a short period of time. This model uses FEA to create a snapshot data map with static inductance, torque, and flux density profile for the SRM as look-up tables. Simulink is used to analyze dynamic behavior, loss distribution and average efficiency of SRM. These two models are coupled in a MATLAB environment to develop a time-efficient model that can be easily modified to suit any SRM configuration. One of the key attributes of this approach is that it does not require the use of a transient FEA software, which can allow one to use open-source software such as FEMM® to analyze the complete dynamic behavior of any SRM drive.

II. ELECTROMAGNETIC ANALYSIS OF HRSRM

In this study, a 6/10 SRM prototype is utilized to perform the modeling process. The overall modeling process and calculation is shown in Fig. 1. The proposed approach includes a core loss estimation model using the iGSE (improved generalized Steinmetz equation) approach [20], which can be used for core loss estimation in time domain.

2021 IEEE Transportation Electrification Conference & Expo (ITEC) | 978-1-7281-7583-6/21/$31.00 ©2021 IEEE | DOI: 10.1109/ITEC51675.2021.9490084

To establish a behavioral model of the machine, the relation between inductance vs. position and static torque vs. current is captured for various magnitudes of current. In addition, a look-up table for average flux density for both stator and rotor tooth and yoke are extracted using finite element analysis towards core loss calculation. These look-up tables can either be obtained from FEA software tools such as ANSYS Electronics, where a transient parametric analysis with a sweep of different current for one electrical cycle by MATLAB code is saved in multiple look-up tables. These results are stored in mat-file for Simulink model to perform dynamic analysis, which are called by MATLAB code as well. This is used to extract inductance and torque at different rotor position from fully unaligned position to the next fully unaligned position. Alternately, inductance and torque profiles can be obtained from hardware measurement, which could be used to develop a hardware-sensitive model. Fig. 2 shows the motor and flux density distribution in the target 6/10 SRM. The static inductance and torque are shown Fig. 3. In addition, a look-up table for average flux density for both stator and rotor tooth and yoke is extracted using finite element analysis towards core loss calculation. The flux density plots for the target HRSRM are shown in Fig. 4.

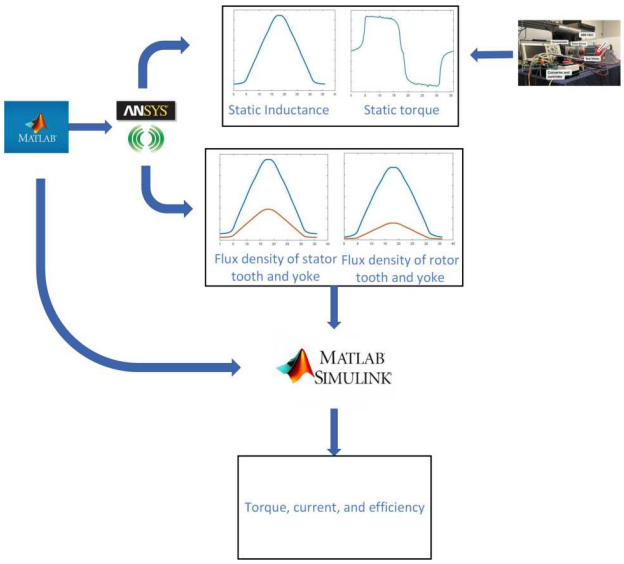

Fig. 1. Proposed dynamic modeling approach

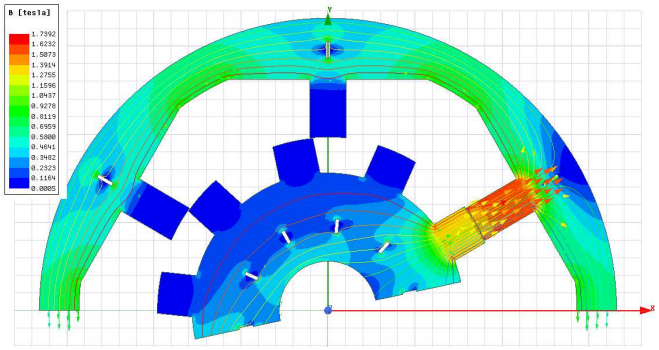

Fig. 2. FEA model for target 6/10 SRM in ANSYS

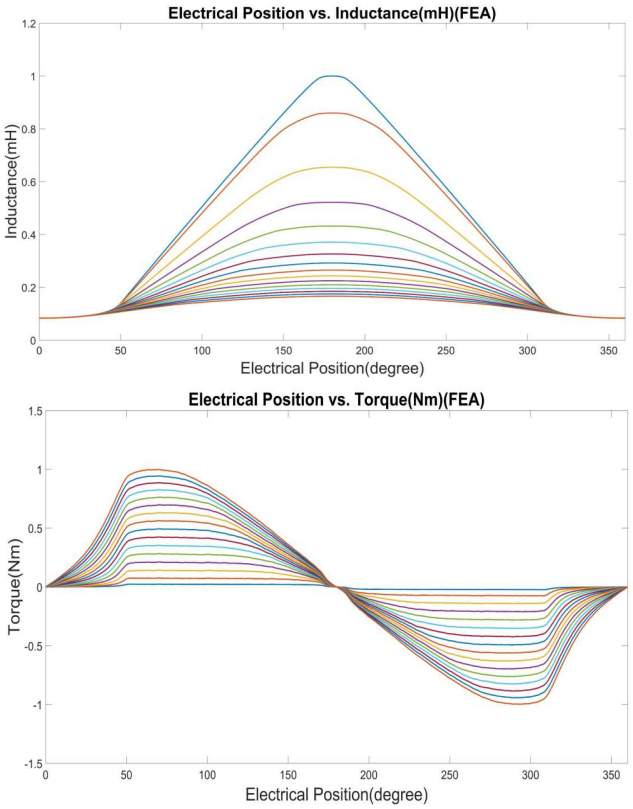

Fig. 3. Normalized FEA results of inductance and torque

III. Proposed Dynamic Behavioral Modeling Approach

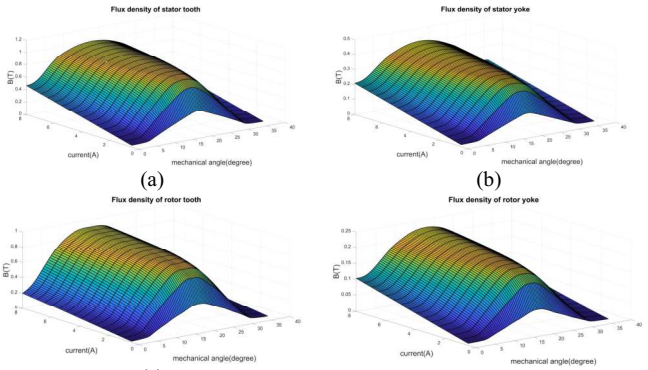

Fig. 4. Normalized flux density map of the HRSRM: (a) stator tooth, (b) stator yoke, (c) rotor tooth, (d) rotor yoke

In the proposed modeling approach, the flux density waveform of each rotor teeth needs to be calculated, which are shown in Fig. 6 and 7. The core losses can be difficult to obtain in the SRM due to the presence of flux densities with various frequencies in different segments on the motor. Therefore, the flux is analyzed segmentally, and the segmentation is shown in Fig. 5. The way to obtain the flux density waveforms of each part on stator is nearly the same with the 6/4 SRM [1]. First, the flux density waveform of stator tooth is obtained by finding the value in the average flux density-current-position look-up table:

$$B_1 = B_{stator\,tooth}(i_{A,}\,\theta_A) \quad (1)$$

$$B_2 = B_{stator\,tooth}(i_{B,}\,\theta_B) \quad (2)$$

$$B_3 = B_{stator\,tooth}(i_{C,}\,\theta_C) \quad (3)$$

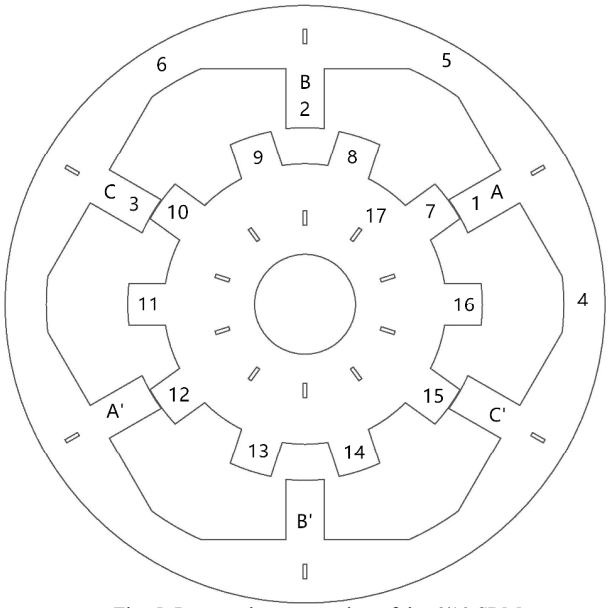

Fig. 5. Proposed segmentation of the 6/10 SRM

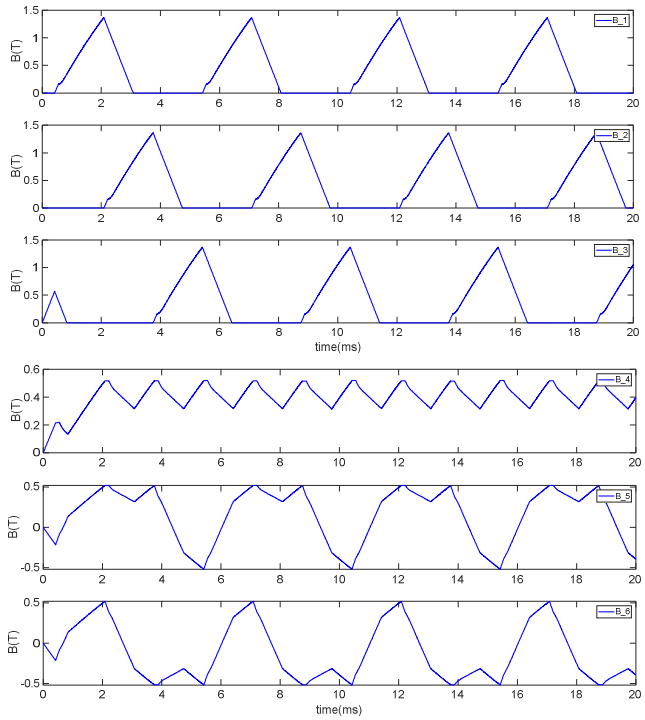

Fig. 6. The flux density waveforms of stator

The waveforms of stator tooth flux density are shown in Fig. 6 (top 3). Then, for stator yoke, the flux density waveform can be derived by adding or subtracting the flux density waveform of stator yoke, which can be targeted in the look-up table of average flux density of stator yoke:

$$B_4 = B_{stator\,yoke}(i_{A,}\,\theta_A) + B_{stator\,yoke}(i_{B,}\,\theta_B) + B_{stator\,yoke}(i_{C,}\,\theta_C) \quad (4)$$

$$B_5 = B_{stator\,yoke}(i_{A,}\,\theta_A) + B_{stator\,yoke}(i_{B,}\,\theta_B) - B_{stator\,yoke}(i_{C,}\,\theta_C) \quad (5)$$

$$B_6 = B_{stator\,yoke}(i_{A,}\,\theta_A) - B_{stator\,yoke}(i_{B,}\,\theta_B) - B_{stator\,yoke}(i_{C,}\,\theta_C) \quad (6)$$

The reason to do this is the static flux density waveform of stator yoke is proportinal to the stator tooth flux denisty waveform. Fig. 6 (bottom 3 figures) shows the waveforms of stator yokes. Owing to symmetry, the flux density wavforms of the other half of the stator are identical to the all waveforms described in Fig. 6 in oppsite direction.

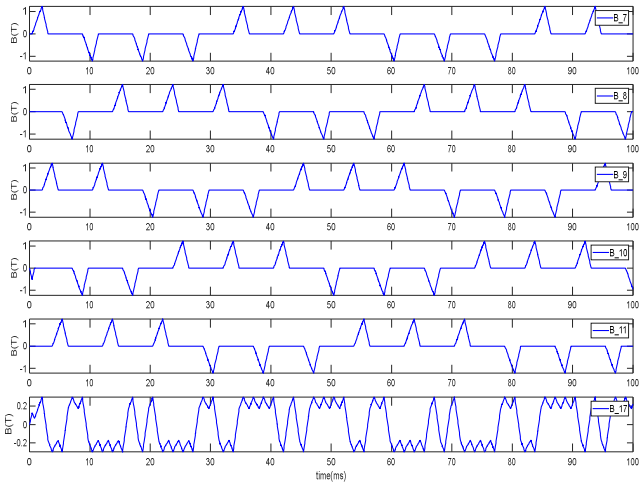

Fig. 7. The flux density waveforms of rotor

The proposed approach relies on reconstructing the flux density in each segment of the rotor, which can be unique for an HRSRM in comparison to a conventional SRM. For a conventional SRM with lower numer of rotor poles, when one rotor tooth moves from aligned position to unaligned position, the adjacent rotor tooth moves from unaligned to aligned position. In other words, a shift between waveforms of two adjacent rotor teeth occurs over one stroke in the conventional SRM. However, for a 6/10 SRM, when one rotor tooth moves from aligned to unaligned position, the flux flows through the rotor tooth two poles away from the first tooth instead of going through the adjacent rotor tooth.

Let us analyze the waveforms of rotor teeth illustrated in Fig. 7. Segment numbers referenced in the geometry of the machine shown in Fig. 5 are used to explain the process. Flux is generated in segment 1 of the machine when phase A is excited, and the flux decays to zero once phase A is turned off. While phase A is on, the flux flows through segments A - 7 – 12 – A'. With the rotor spining, segments 9 & 14, 11 & 16, 13 & 8, and 15 & 10 are activated sequentially. Segment 9 has a delay of one stroke with respect to segment 7. Segment 8 is adjacent to segment 7, and is delayed by 3 strokes w.r.t. segment 7. The values of the waveforms depend on the static average flux density profile in the rotor tooth for the specific current and position. The waveform for flux density in segments 7 – 11 are shown is Fig. 7. Once again, because of the symmetry, the flux density waveforms of the

other half of the rotor is identical to the waveforms described in Fig. 7, just in the opposite direction.

After the waveforms of rotor tooth flux density are identified, the flux density waveforms of rotor yoke are easier to obtain. Since the static flux density waveform of rotor yoke is proportional to the waveform of rotor tooth, for example in part 17 of Figure 5, the waveform is proportional to $B_7 + B_8 - B_9 + B_{10} - B_{11}$, and the values are dependent on the curve of static average rotor yoke flux density, which is shown in Fig. 7 as well.

For analyzing dynamic performance and efficiency simultaneously, iGSE is most suitable for core loss analysis and yields very accurate results. The generalized iGSE equation is given as:

$$P_{total\_core}(t) = k_i \left|\frac{dB}{dt}\right|^{\alpha} (\Delta B)^{\beta-\alpha} \tag{7}$$

where

$$k_i = \frac{k}{(2\pi)^{\alpha-1} \int_0^{2\pi} |\cos\theta|^{\alpha} 2^{\beta-\alpha} d\theta} \tag{8}$$

where k is the coefficient for hysteresis loss (k_h), eddy current loss (k_c), and excess loss (k_e). α and β are Steinmetz coefficients, for hystersis loss, α =1 and β =2, for eddy current loss, α =2 and β =2, for excess loss, α =1.5 and β =1.5. The generalized iGSE can be written as:

$$P_{total\_core}(t) = k_{ih} \left|\frac{dB}{dt}\right| (\Delta B) + k_{ic} \left|\frac{dB}{dt}\right|^2 + k_{ie} \left|\frac{dB}{dt}\right|^{1.5} \tag{9}$$

where k_{ih}, k_{ic}, and k_{ie} can be calculated using the formula above, the k in these cases are coefficient k_h, k_c, and k_e, which can be obtained by the iron loss model under sinusoidal flux density waveforms by curve fitting. ΔB represents the peak-to-peak value of a non-sinusoidal flux density waveform of both major hysteresis loop and minor hysteresis loop. Therefore, the waveforms of SRM for each parts are seperated into majar loop and minor loop. The formula mentioned above is used to calculate the loss density, so the total loss of the SRM is the sum of products of volume of each part of machine and the loss density.

The motor model was integrated in Simulink with the electromagnetic map model to develop the behavioral model towards evaluation of the performance, efficiency, and design advanced power electronics control and sensorless algorithms. In this study, an asymmetric bridge converter with current hysteresis control was used to control the SRM. The block diagram of Simulink system is shown in Fig. 8. The eletromagentic torque mdoelling part of this system is basically based on dynamic phase equation of SRM:

$$L(\theta, i)\frac{di_{ph}}{dt} = V_{dc} - R_s i_{ph} - \frac{dL(\theta, i)}{dt} i_{ph} \tag{10}$$

where i_{ph}, $L(\theta, i)$, R_s are the phase current, inductance, resistance and V_{dc} is the DC bus voltage.

The efficiency calculation utilizes Ohmic loss and core loss which is discussed above:

$$\eta_{SRM} = \frac{P_{in} - P_{ohmic} - P_{core}}{P_{in}} \tag{11}$$

where core loss is time average value.

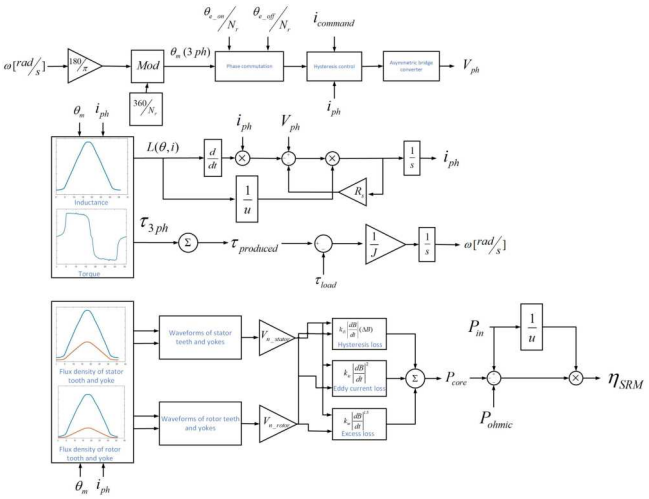

Fig. 8. FEA model for target 6/10 HRSRM in ANSYS

IV. Simulation Results and Experimental Verifiction

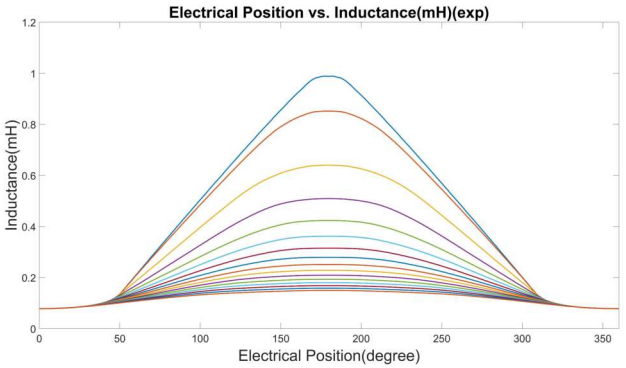

Fig. 9. Normalized (experimental) inductance map

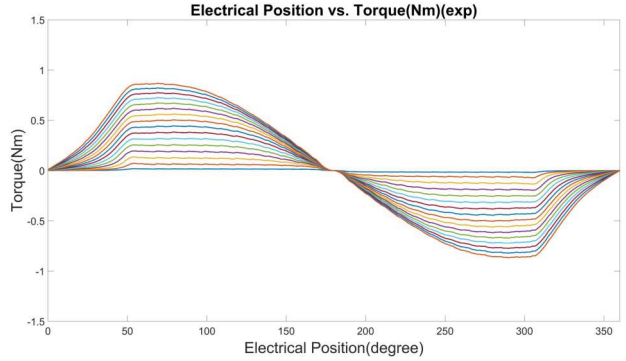

Fig. 10. Normalized (experimental) torque map

To verify accuracy of the proposed model, FEA simulations from ANSYS Electronics software were compared with hardware measurements for torque and inductance from experimental setup, which is shown in Fig. 9 and 10. The hardware setup is shown in Fig. 11. The dynamic behaviors are compared, for comparing the dynamic performance analysis, the simulations are done for 900 RPM, the firing angle for the controller is 30 – 150 electrical degree, the voltage source is 680V DC link. The results are compared with both FEA and experiment. Since the sampling frequency is different for the two sitautions, they are compared seperately, and shown in Fig. 12 and 13.

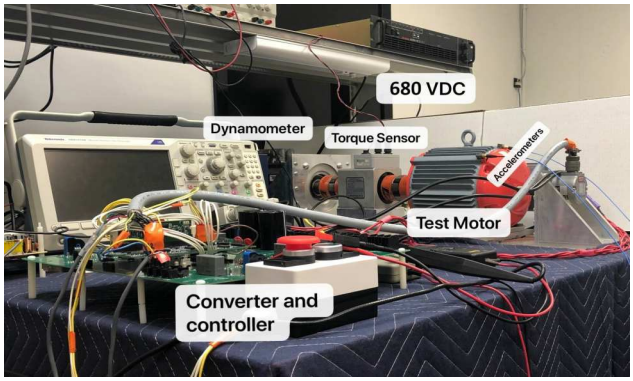

Fig. 11. Experimental setup for the target SRM

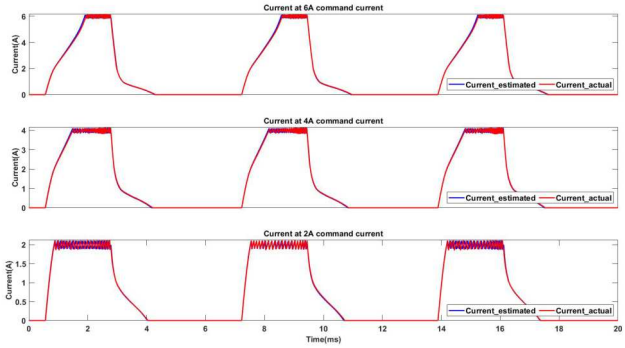

Fig. 12. FEA and simulated phase currents

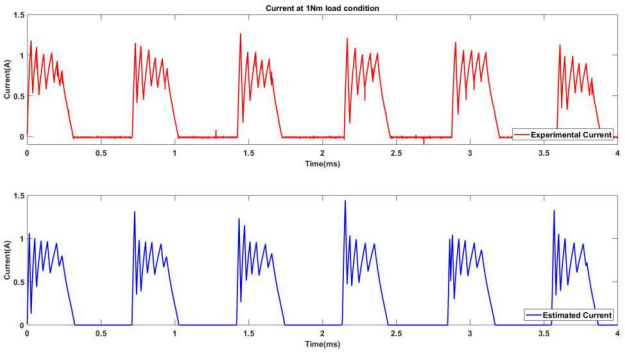

Fig. 13. Experimentally measured (top) and simulated (bottom) phase currents

Fig. 14 and 15 show the core loss comparison for 600 rpm and 900 rpm respectively. The maximum error are 1.8 W and 1.4 W respectively for two cases, which clearly shows the accuracy of proposed model is comparable to FEA simulation.

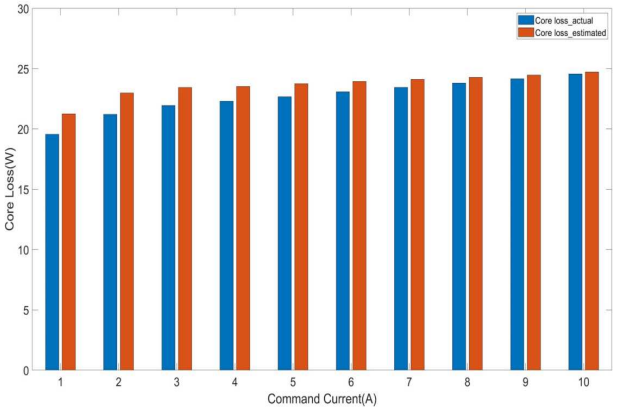

Fig. 14. Core loss comparison at 600 rpm

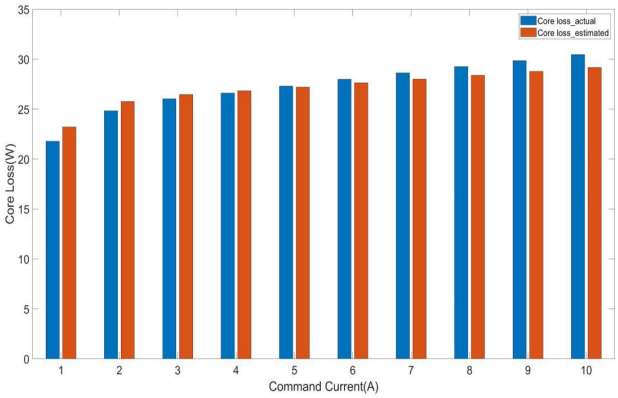

Fig. 15. Core loss comparison at 900 rpm

V. Conclusion

This paper presents a hybrid behavioral modelling approach for SRMs with particular emphasis on high rotor pole SRMs. This modelling technique is created to analyze the dynamic behavior of SRM efficiently in term of simulation time and computation resource for multiple operating points simluation, in the meanwhile without sacrifice of the accuracy. The simulation and experimental results are compared in dynamic current and core loss, which validates the accuracy of this model. Although the model has been studied for a 6/10 SRM, this technique can be used for dynamic behavior analysis and controller design for other types of SRM with minor modifications.

ACKNOWLEDGMENT

This work was supported in part by the U.S. National Science Foundation under Grant 1927432 and by Turntide Technologies.

REFERENCES

[1] Krishnan, R., Switched reluctance motor drives: modeling, simulation, analysis, design and applications, Boca Raton, FL: CRC P, 2001.
[2] T. J. E. Miller, Switched Reluctance Motor and Their Control. Lebanon, OH, USA: Magna Physics Publishing, 1993.
[3] D.W. J. Pulle, "New data base for switched reluctance drive simulation," IEEE Proc.-B, vol. 138, no. 6, pp. 331–337, Nov. 1991.
[4] D. A. Torrey and J. H. Lang, "Modeling a nonlinear variable-reluctance motor drive," IEE Proc. B- Elect. Power Appl., vol. 137, no. 5, pp. 314–326, Sept. 1990.
[5] W. M. Chan and W. F. Weldon, "Development of a simple nonlinear switched reluctance motor model using measured flux linkage data and curve fit," in Proc. IEEE IAS Annu. Meeting, New Orleans, LA, USA, 1997, pp. 318–325.
[6] V. Nasirian, S. Kaboli, A. Davoudi, and S. Moayedi, "High-fidelity magnetic characterization and analytical model development for switched reluctance machines," IEEE Trans. Magn., vol. 49, no. 4, pp. 1505–1515, Apr. 2013.
[7] Z. Jin, Y. Jia, M. Salameh, B. Bilgin, S. Li and M. Krishnamurthy, "A Truncated Fourier Based Analytical Model for SRMs with Higher Number of Rotor Poles," 2020 IEEE Transportation Electrification Conference & Expo (ITEC), Chicago, IL, USA, 2020, pp. 1044-1049, doi: 10.1109/ITEC48692.2020.9161708.
[8] R. Arumugam, D. A. Lowther, R. Krishnan, and J. F. Lindsay, "Magnetic field analysis of a switched reluctance motor using a two dimensional finite element method," IEEE Trans.Magn., vol.MAG-21, no. 5, pp. 1883–1885, Sept. 1985.
[9] B. Parreira, S. Rafael, A. J. Pires, and P. J. C. Branco, "Obtaining the magnetic characteristics of an 8/6 switched reluctance machine: From FEM analysis to the experimental tests," IEEE Trans. Ind. Electron., vol. 52, no. 6, pp. 1635–1643, Dec. 2005.
[10] K. Kiyota, T. Kakishima, H. Sugimoto, and A. Chiba, "Comparison of the test result and 3D-FEM analysis at the knee point of a 60 kW SRM for a HEV," IEEE Trans. Magn., vol. 49, no. 5, pp. 2291–2294, May 2013.
[11] Q. Yu and D. Gerling, "Analytical modeling of a canned switched reluctance machine with multilayer structure," IEEE Trans. Magn., vol. 49, no. 9, pp. 5069–5082, Sep. 2013.
[12] J. C. Moreira and T. A. Lipo, "Simulation of a four-phase switched reluctance motor including the effects of mutual coupling," Electric Machines and Power Systems, vol. 16, no. 4, pp. 281–299, 1989.
[13] R. M. Davis and I. Al-Bahadly, "Experimental evaluation of mutual inductances in a switched reluctance motor," Int. Conf. Power Electron. Variable-Speed Drives, London, UK, 1990, pp. 243-248.
[14] M. A. Preston and J. P. Lyons, "A switched reluctance motor model with mutual coupling and multi-phase excitation," IEEE Trans. Magn., vol. 27, no. 6, pp. 5423–5425, Nov. 1991.
[15] T. Sawata et al., "Multi-dimensional, non-linear, lumped magnetic circuit for dynamic modeling of mutual coupling and faults in switched reluctance motors," 8th EPE, Brussels, Belgium, pp. 1–7, Sep. 1999.
[16] C. S. Edrington, B. Fahimi and M. Krishnamurthy, "An Autocalibrating Inductance Model for Switched Reluctance Motor Drives," in IEEE Transactions on Industrial Electronics, vol. 54, no. 4, pp. 2165-2173, Aug. 2007.
[17] A. Kechroud, J. J. H. Paulides, and E. A. Lomonova, "B-spline neural network approach to inverse problems in switched reluctance motor optimal design," IEEE Trans. Magn., vol. 47, no. 10, pp. 4179–4182, Oct. 2011.
[18] B. Bilgin, A. Emadi and M. Krishnamurthy, "Design considerations for switched reluctance machines with higher number of rotor poles for solar-assisted plug-in electric auto rickshaw," 2010 IEEE International Symposium on Industrial Electronics, Bari, 2010, pp. 1247-1252.
[19] P. C. Desai, M. Krishnamurthy, N. Schofield and A. Emadi, "Novel Switched Reluctance Machine Configuration with Higher Number of Rotor Poles Than Stator Poles: Concept to Implementation," in IEEE Transactions on Industrial Electronics, vol. 57, no. 2, pp. 649-659, Feb. 2010.
[20] Kapil Venkatachalam, Charles R. Sullivan, Tarek Abdallah, and Hernan Tacca, "Accurate Predication of Ferrite Core Loss with Nonsinusoidal Waveforms Using Only Steinmetz Parameters", in COMPEL 2002: 8th IEEE Workshop on Computers in Power Electronics.